Chats 2019
Applied Superconductivity

Field Quality Analysis in the HTS Dipole Insert-Magnet Feather M2 with the Finite Element Method

09-12 July 2019

L. Bortot[1,2], M. Mentink[1], C. Petrone[1],
S. Schöps[2], J. Van Nugteren[1], A. Verweij[1]

1 CERN
2 TECHNISCHE UNIVERSITÄT DARMSTADT

(*) ce
(**) Bundesministerium für Bildung und Forschung

This work is supported by:
(*) The 'Excellence Initiative' of the German Government and by the Graduate School of Computational Engineering at TU Darmstadt;
(**) The Gentner program of the German Federal Ministry of Education and Research (grant no. 05E12CHA).

High-Temperature Superconductors

Cuprate compounds (CuO_2) doped with rare earth elements (La, Bi-Sr-Ca, Y-Ga-Ba …)

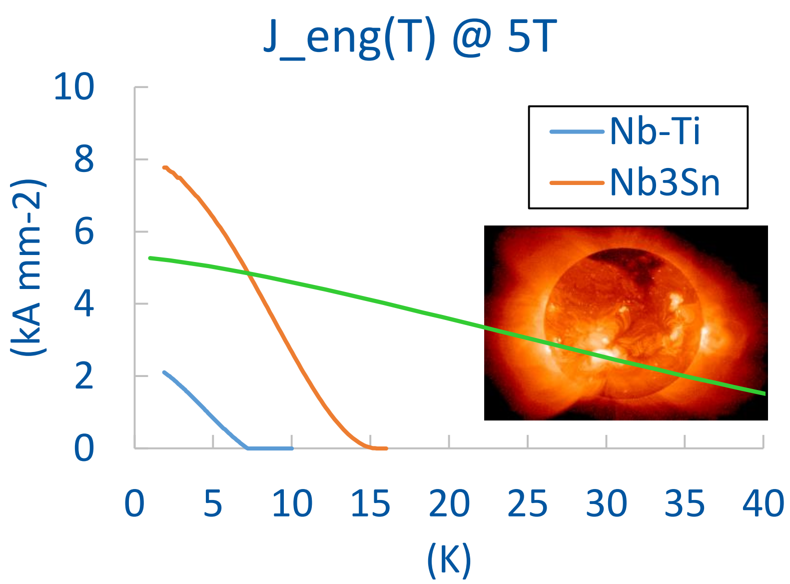

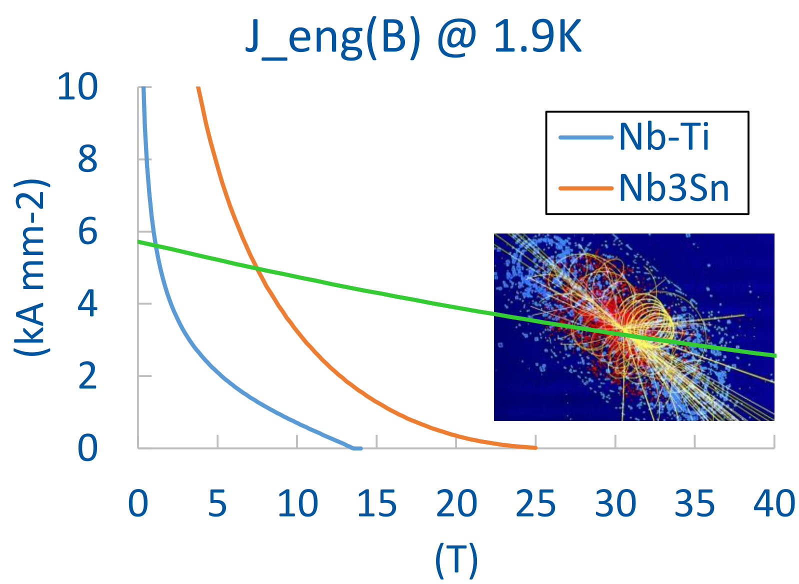

- Higher Tc and Bc0 respect to the traditional low-temperature superconductors (LTS)
- Higher performance comes with higher prices! $\$_{\text{HTS}} \approx 1e^2\ \$_{\text{LTS}}$

.. But in the early 2000s it was $\approx 1e^3$

Outline

A. **Introduction**

B. **Motivation**

C. **Formulation**

D. **Verification**
   Theoretical references

E. **Validation**
   Measurements from Feather2

F. **Summary and Outlook**

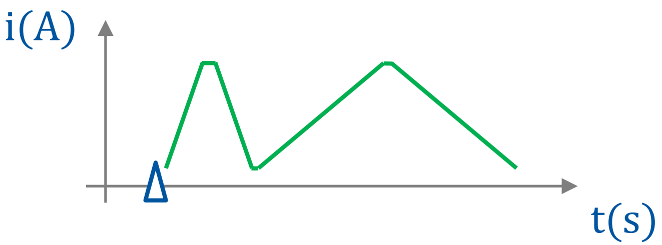

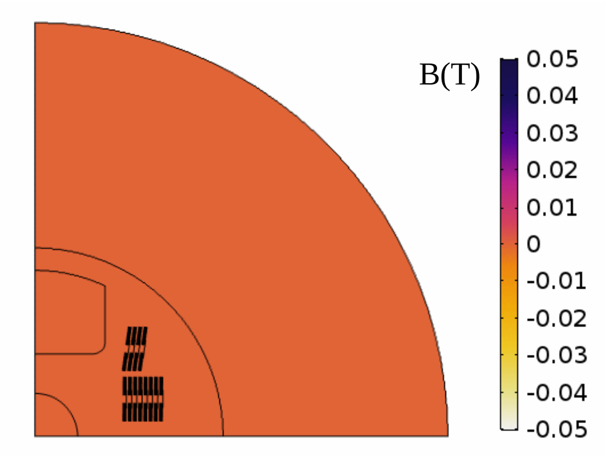

Feather2 magnet: net magnetic flux density contribution due to screening currents (first quadrant)

Introduction: Field Quality

Magnet aperture Ω_a
2D magnetostatic field $\nabla^2 A_z = 0$

General Solution: Fourier expansion series

$$B_r(r,\varphi) = \sum_{n=1}^{\infty} \underbrace{n r^{n-1} \gamma_n}_{A_n(r)} \cos(n\varphi) + \underbrace{n r^{n-1} \delta_n}_{B_n(r)} \sin(n\varphi)$$

- $A_n(r)$, $B_n(r)$ live on boundary Γ_a
- skew and normal magnetic field multipoles
- Determined by measurements (rotating coil)

Distortion Factor (metrics for field quality)

$$F_{d,1}(r_0) = \frac{1}{B_1(r_0)} \sqrt{\sum_{n=2}^{k} [A_n(r_0)^2 + B_n(r_0)^2]}$$

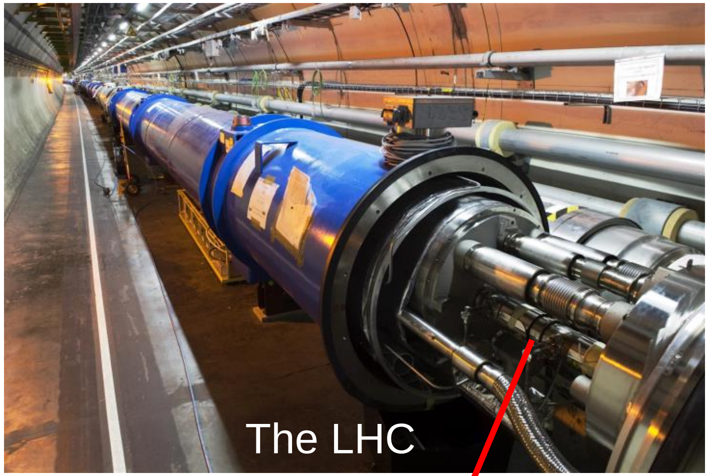

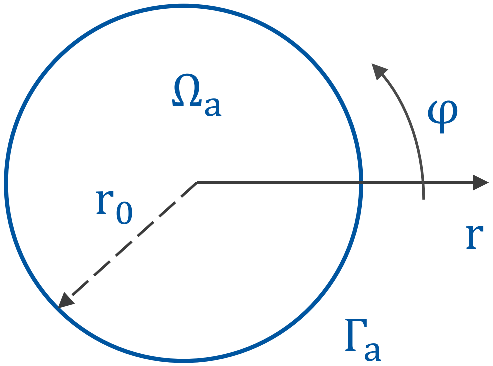

Cross section of the beam pipe

Introduction: Field Multipoles

Normal field multipoles for the reference circumference $r_0 = 1\ \mathrm{m}$

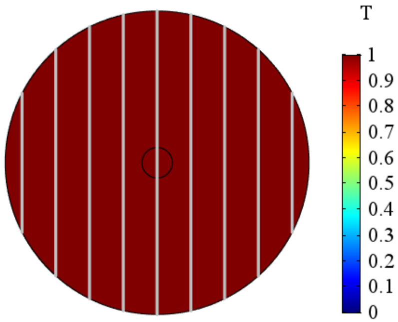

B_1 dipole

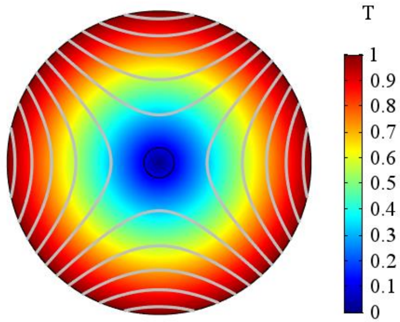

B_2 quadrupole

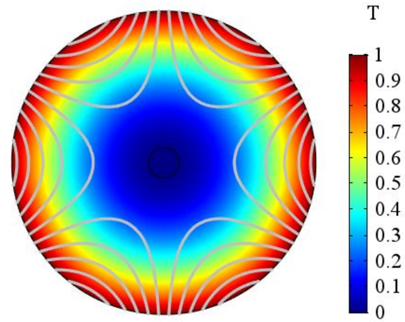

B_3 sextupole

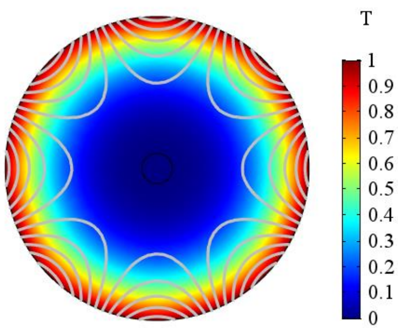

B_4 octupole

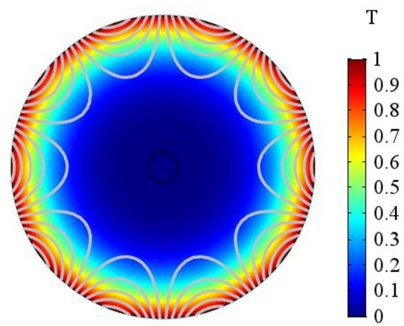

B_5 decapole

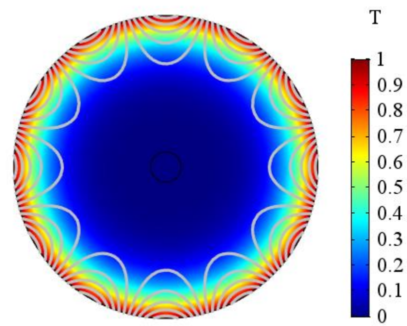

B_6 dodecapole

Introduction: Screening (Eddy) Currents

ReBCO tape in an external magnetic density $\vec{B}$:

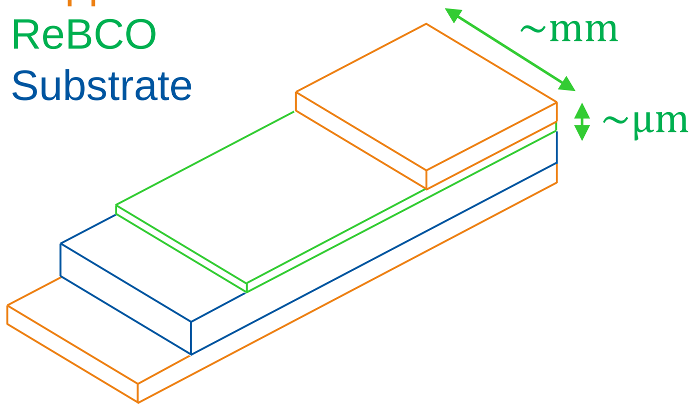

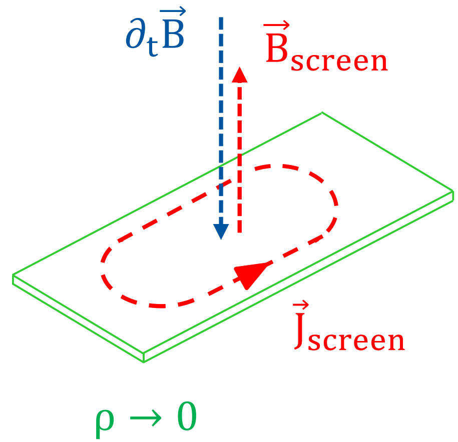

- Magnetic field variation $\partial_t \vec{B}$: → Screening currents $\vec{J}_{screen}$
- $\rho \rightarrow 0$ → Persistent magnetization $\vec{B}_{screen}$

- Large filament size (4~12 mm), significant persistent magnetization:
  - Field quality, especially at low field
  - Thermal behavior, principal Joule loss contribution

Motivation

Design of future HTS magnets for accelerators

- Screening currents dynamics shall be taken into account
- Field error due to screening currents shall be corrected, especially at low field

A code with this purpose shall be:

- Numerically stable
- Scalable to accelerator magnets
- Validated, reliable, maintainable

Optionally:

- Capable of field-circuit coupling
- Efficient

Our contribution

- Investigation and extension of a suitable field formulation
- Implementation in a proprietary software (*), using the Finite Element Method
- Scaling of the field formulation to an HTS magnet (Feather2)

(*) COMSOL Multiphysics® v. 5.3. www.comsol.com. Last access: 01/07/2019

Formulation: 1) Mixed Fields

Mixed potentials

- Domain decomposition
- $\vec{A}$ solved in Ω_A (air, iron), where $\sigma \to 0$
- $\vec{H}$ solved in Ω_H (conductors), where $\rho \to 0$:
- T soved everywhere

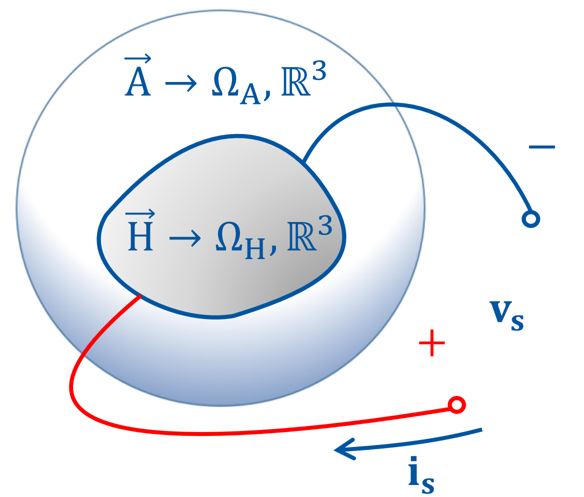

Discrete weak formulation:

$$\begin{bmatrix} \mathbf{K}^{\nu} + \mathbf{M}^{\sigma}\frac{\mathrm{d}}{\mathrm{dt}} & -\mathbf{Q} & \mathbf{0} & \mathbf{0} \\ \mathbf{Q}^{\top}\frac{\mathrm{d}}{\mathrm{dt}} & \mathbf{K}^{\rho} + \mathbf{M}^{\mu}\frac{\mathrm{d}}{\mathrm{dt}} & -\mathbf{X} & \mathbf{0} \\ \mathbf{0} & \mathbf{X}^{\top} & \mathbf{0} & \mathbf{0} \\ \mathbf{0} & \mathbf{0} & \mathbf{0} & \mathbf{K}^{\mathrm{k}} + \mathbf{M}^{\rho}\frac{\mathrm{d}}{\mathrm{dt}} \end{bmatrix} \cdot \begin{bmatrix} \mathbf{a} \\ \mathbf{h} \\ \mathbf{v}_{\mathrm{s}} \\ \mathbf{t} \end{bmatrix} = \begin{bmatrix} \mathbf{0} \\ \mathbf{0} \\ \mathbf{i}_{\mathrm{s}} \\ \mathbf{P}_{\mathrm{J}} \end{bmatrix}$$

Ampere-Maxwell
Faraday
Heat Balance
Field coupling
Circuit coupling

Finite material properties → bounded condition number → Numerical stability

Formulation: 2) Model Order Reduction

Model order reduction → Speed-up

High aspect ratio

Tapes as surfaces in $\mathbb{R}^3$ (lines in $\mathbb{R}^2$)

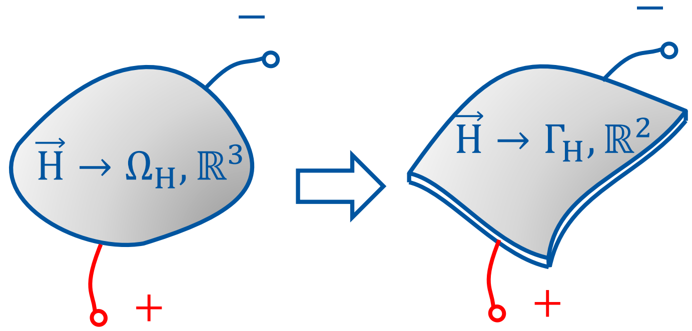

Model order reduction

2D transverse field configuration

Tapes as lines in $\mathbb{R}^2$

Electric field balance in the superconductor

- External E_s ,Resistive E_r, Inductive E_i
- Current sharing resolved with root finding algorithm

with $E_s = -\chi_z v_s$

- χ_z as voltage distribution function
- v_s external voltage supply
  - **Input**, if voltage driven model
  - **Lagrange multiplier**, if current driven model

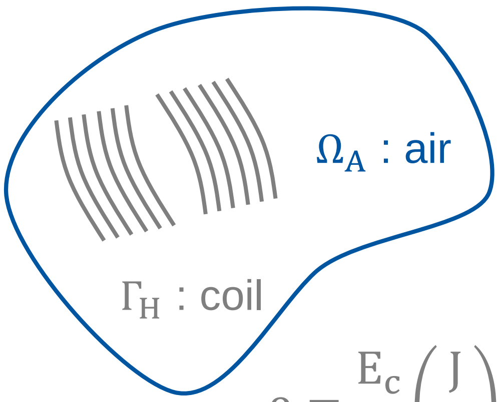

$$\rho = \frac{E_c}{J_c}\left(\frac{J}{J_c}\right)^{n-1}$$

Roebel Cables → Transposition → Even current distribution in the tapes

Outline

A. Introduction

B. Motivation

C. Formulation

D. Verification

Theoretical references

1. Critical State (Bean) Model
2. Skin Effect
3. Field Dependency

E. Validation

F. Summary and Outlook

Verification – 1. Critical State (Bean) Model

Scenario: magnetic field diffusion

$$n_{\mathrm{powerLaw}} = \infty\ (1e^3),\quad \mathrm{J_c} = \mathrm{J_{c0}}$$
$$\rightarrow \rho = \{0; \rho_c\}$$

Geometry: slab of infinite height, modelled as stack of tapes

Source: boundary field $\mathrm{H_s}$

Reference: Analytical solution:

$$\mathrm{H_{sol}}(x,t) = x \cdot \mathrm{J}(x,t)$$
$$\mathrm{J}(x,t) = \{0;\ \pm \mathrm{J_{c0}}(\mathrm{sign}(H))\}$$

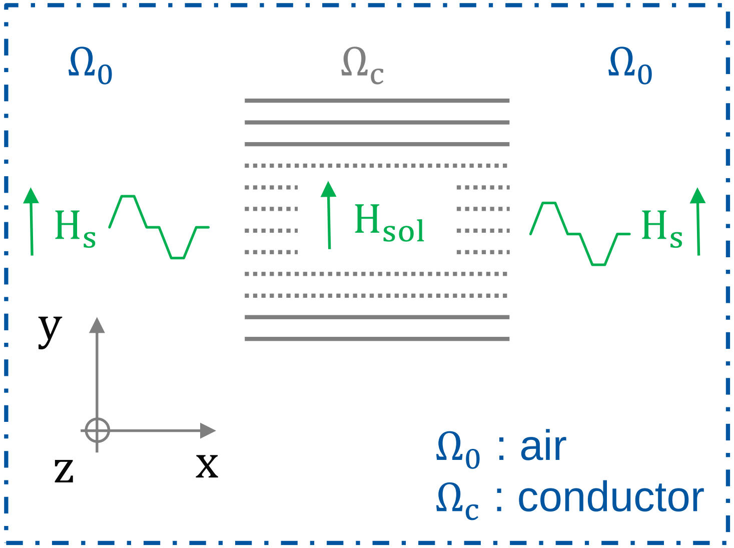

Computational domain

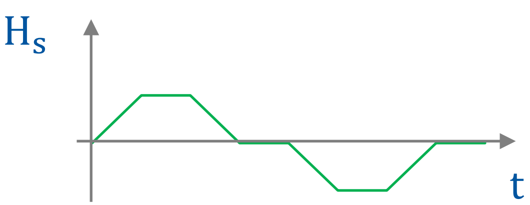

Source term

Verification – 1. Critical State (Bean) Model

Numerical Solution: magnetic field diffusion

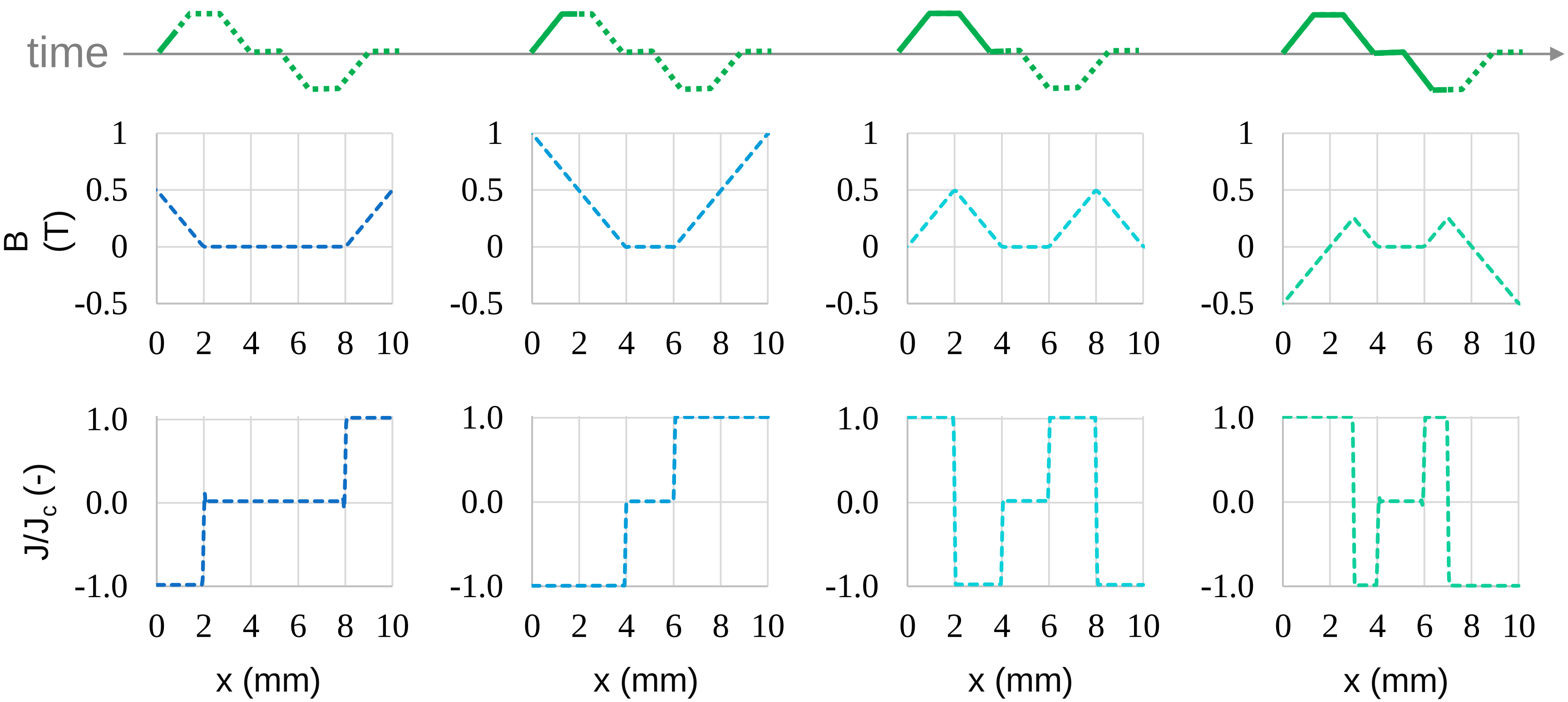

Magnetic flux density and normalized current density distribution

→ Distributions consistent with theory

Verification – 2. Skin Effect

Scenario: magnetic field diffusion

$$n_{\mathrm{powerLaw}} = 1, \quad J_c = J_{c0}$$
$$\rightarrow \rho = \mathrm{const}$$

Geometry: bulk material, modelled as stack of tapes

Source: boundary field H_s

Reference: Analytical solution:

$$H_{sol} = H_s\left(1 - f_{erf}(\xi)\right)$$

$f_{erf}(\xi)$ Gaussian error function

$\xi = \frac{x}{2\sqrt{k(t-t^*)}}$ Similarity variable

$k = \rho\mu_0{}^{-1}$ Magnetic diffusivity

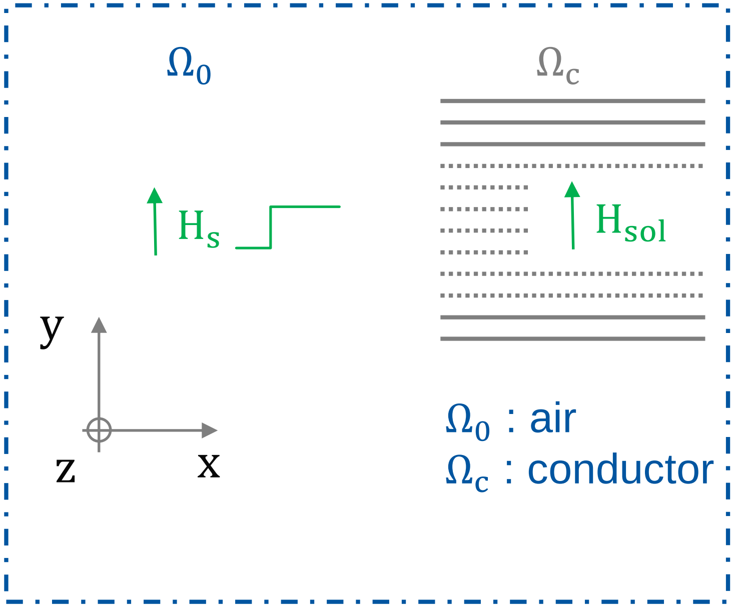

Computational domain

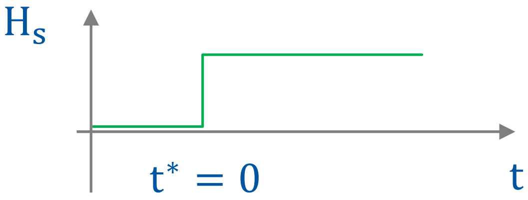

Source term

Verification – 2. Skin Effect

Numerical Solution: magnetic field diffusion

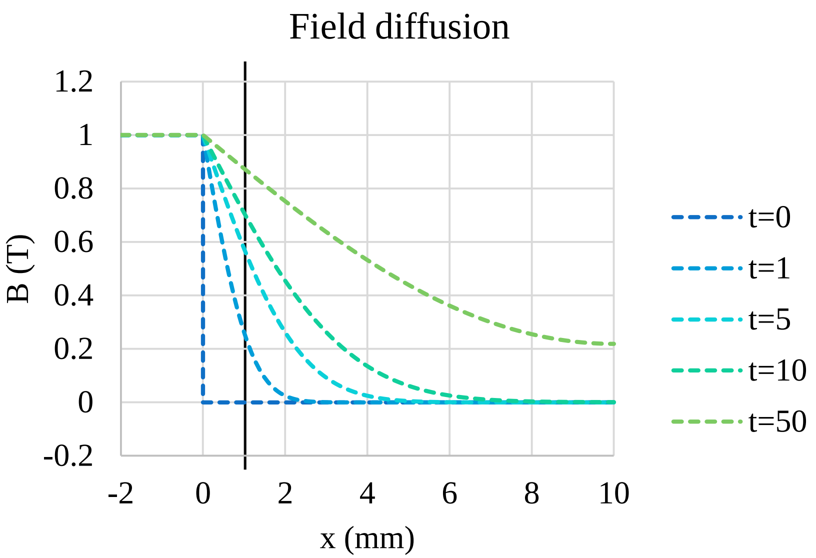

Magnetic flux density distribution
in the conductive slab

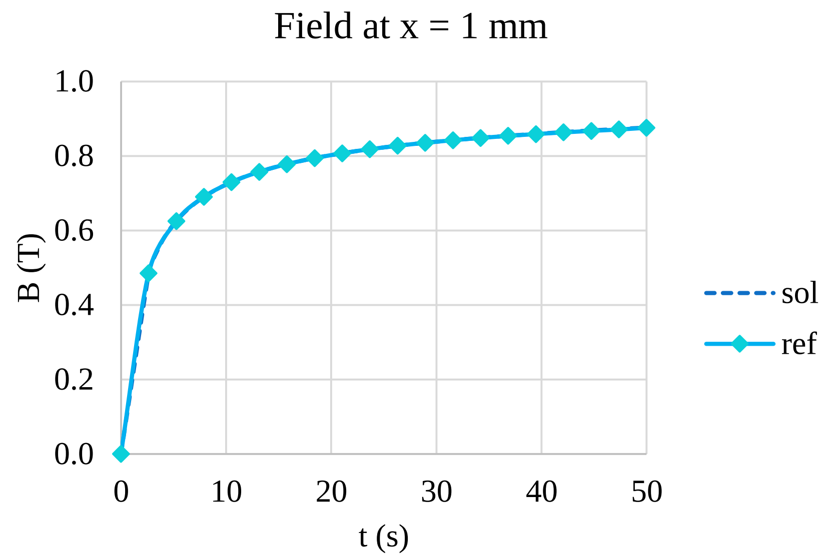

Magnetic flux density distribution
at x=1 mm, as function of time: numerical solution (sol) and analytical solution (ref)

→ Consistent with theory [6]

Verification – 3. Field Dependency

Scenario: AC loss due to screening currents

$1 < n_{\text{powerLaw}} < \infty,\ \ J_c = J_{c0}$

$\rightarrow$ ρ as power law

Geometry: single tape, orthogonal to the field

Source: boundary field H_s

Reference: Analytical solution:
Q_{AC} AC loss (J/cycle), H_p penetration field

if $H < H_p$: $Q_{AC} \propto H^4, Q_{AC} \propto f^0$

if $H > H_p$: $Q_{AC} \propto H^1$

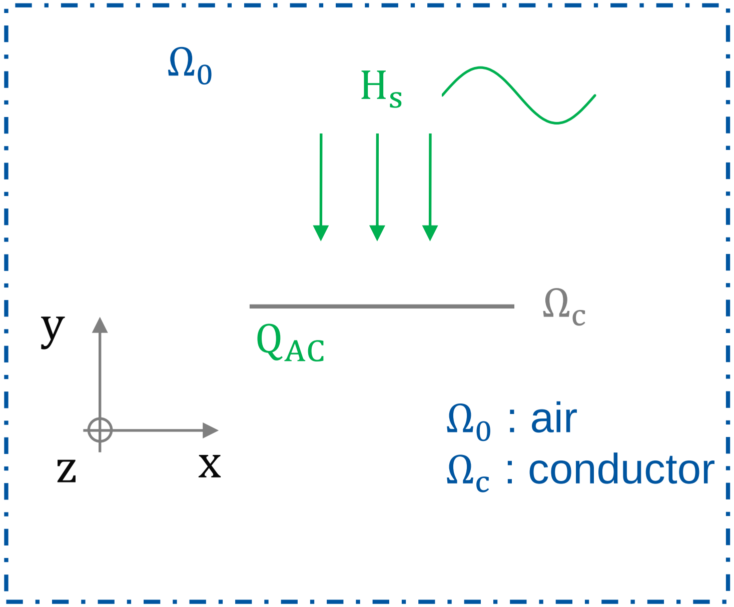

Computational domain

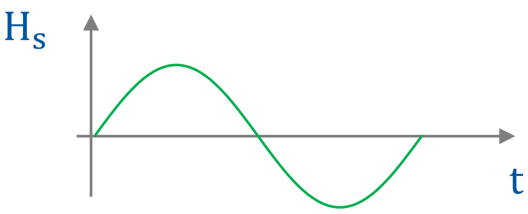

Source term

Verification – 3. Field Dependency

Numerical Solution: AC loss due to screening currents

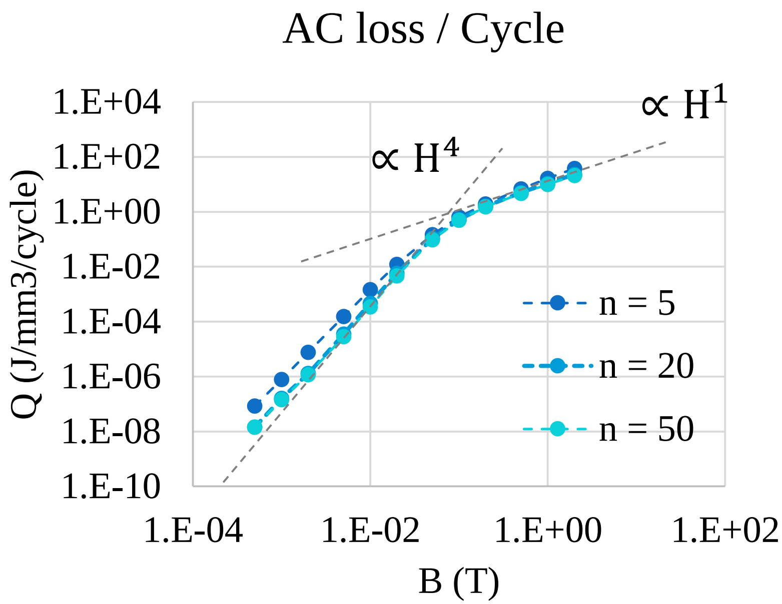

Ac loss per cycle, as function of the applied field

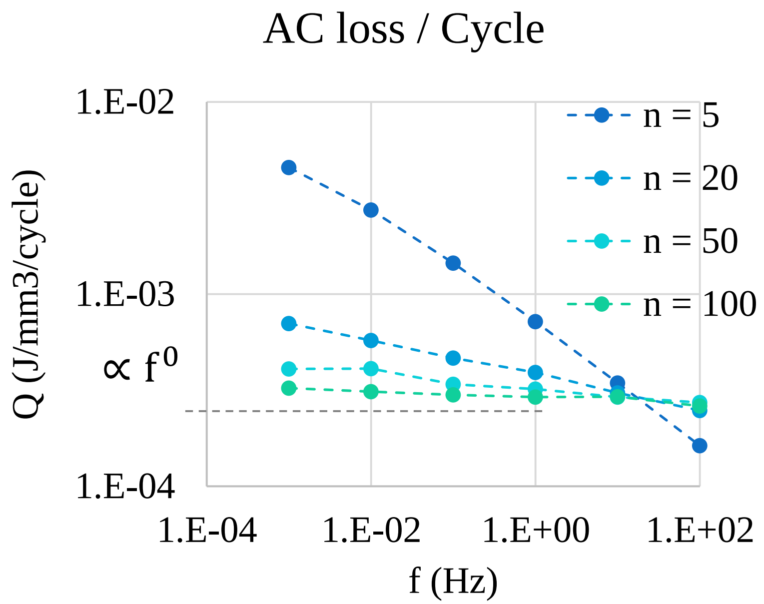

Ac loss per cycle, as function of frequency, for $H < H_p$

→ Consistent with theory

Outline

Crosscheck

Reference model based on the $\vec{H}$ formulation, available at http://www.htsmodelling.com

HTS MODELLING WORKGROUP

2D model of a Single HTS tape in self-field

Source: $I_s = I_0 \sin(2\pi f t)$, $I_0 = 2I_{crit}$ $t \in [0; 1]$

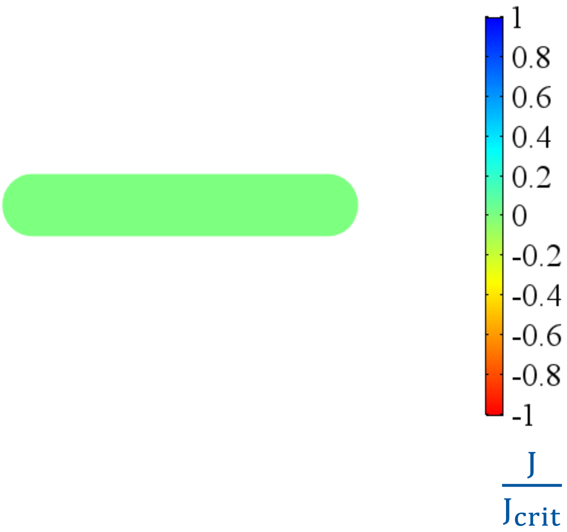

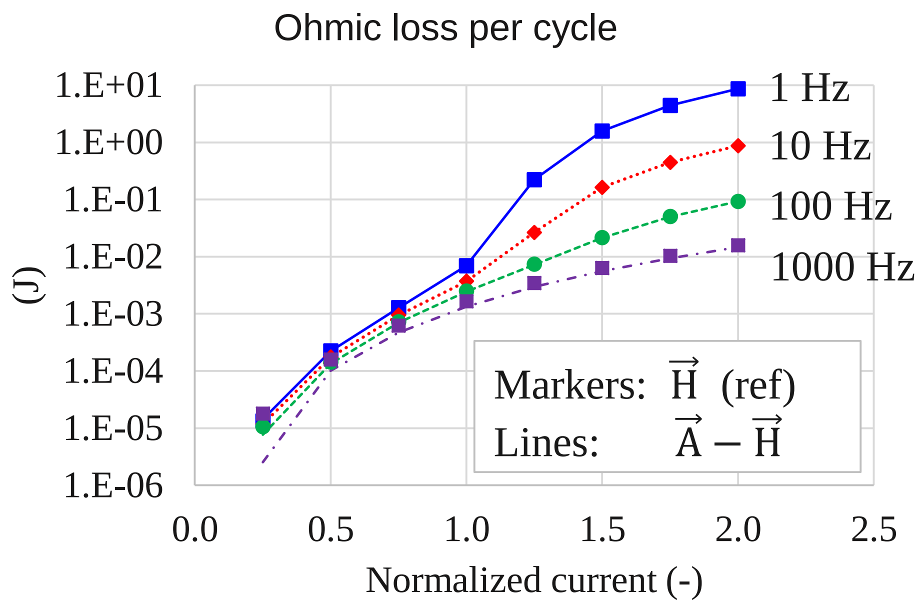

Benchmark

Forecasts on expected computational time:

Same physics…

1 tape

5 tapes

10 tapes

Increased computational cost

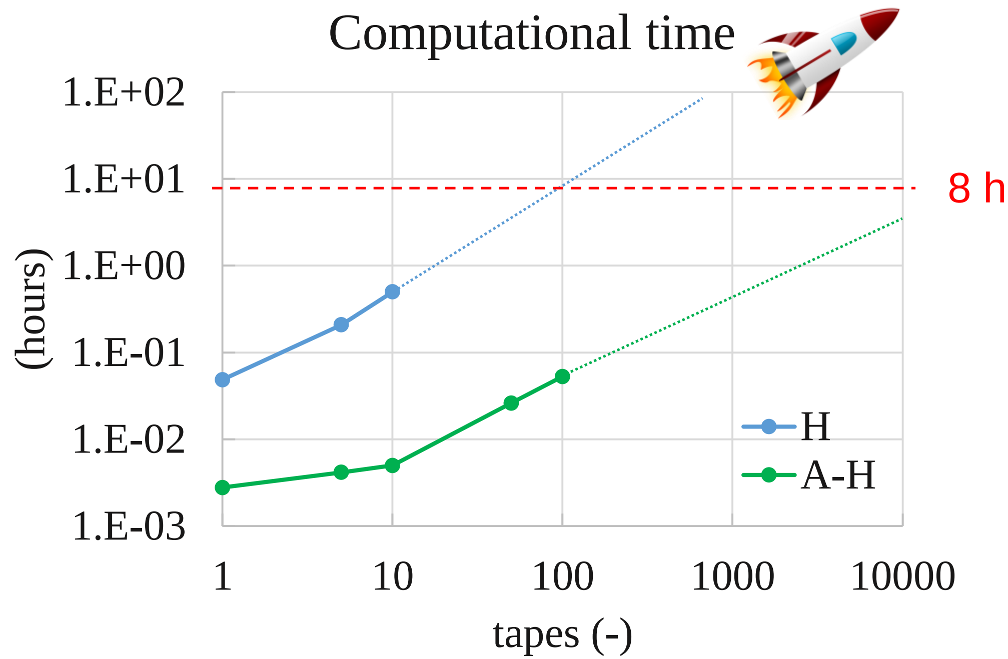

CPU: Intel Core i7-3770 @ 3.40GHz. RAM: 32 Gb. OS: Win 10

Feather2 Dipole Insert Magnet

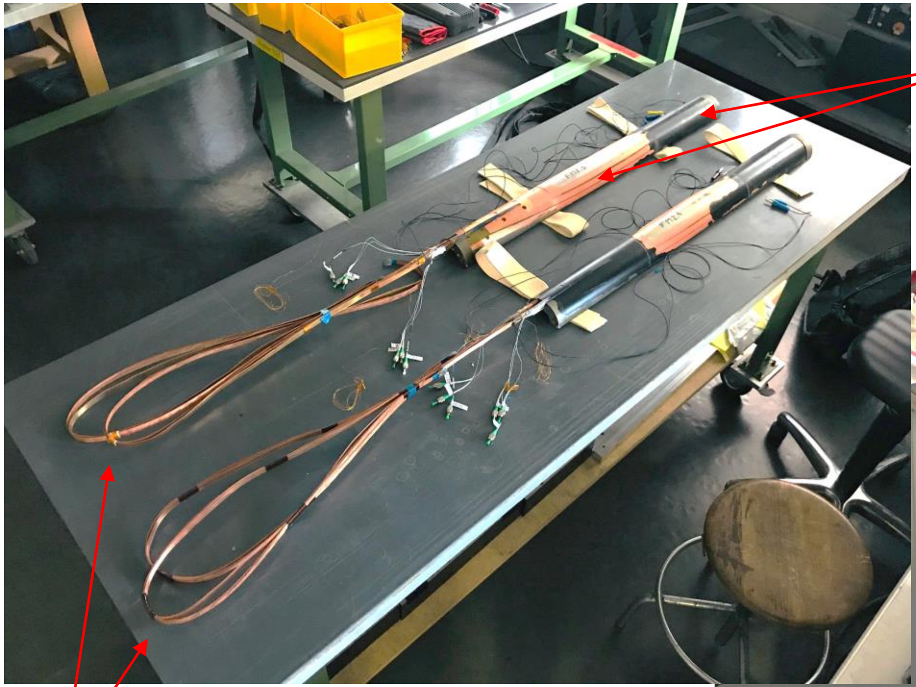

Central and wing decks, for upper and lower coils

External support cylinder

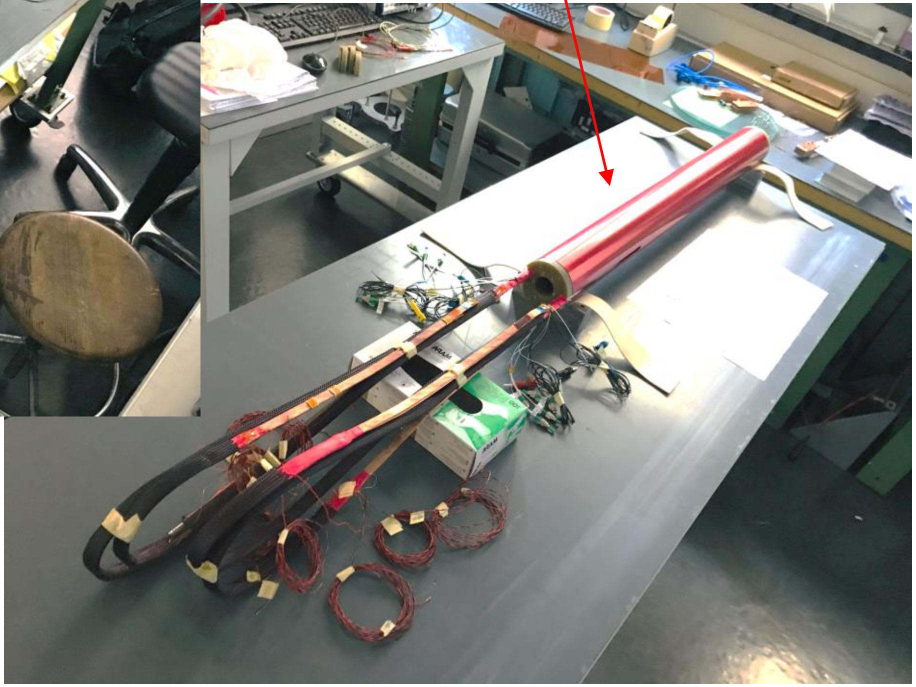

Current leads

Courtesy of J. Van Nugteren

Measurements on Feather2

Scenario: magnetic field quality in the Feather M2 insert dipole magnet

$n = 20, \; J_c(T, B, \theta)$

→ ρ as anisotropic power law, derived from data @ 77 K

Uncertainty in material properties

Geometry: tapes modelled as lines

Source: measured current

Reference: measurements carried out by *C. Petrone* (CERN)

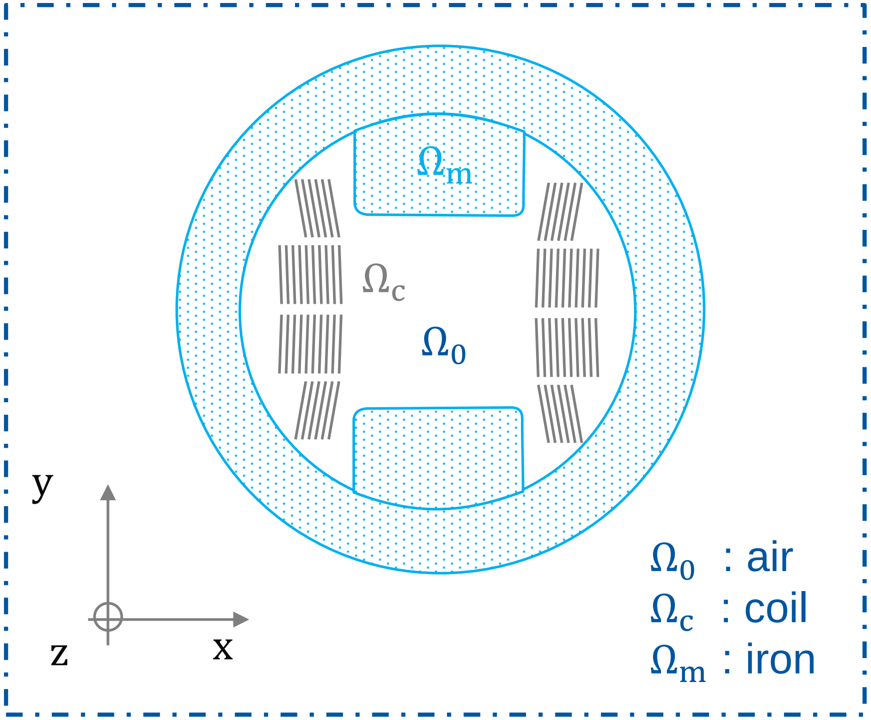

Computational domain

Modelling of Jc (T, B, θ)

- J_c available only for $T = 77\ K$ → Need for a lift factor
- Calibrated with the measured critical current I_c
- Gauged with $\theta = 30°$ (magnetostatic simulation)

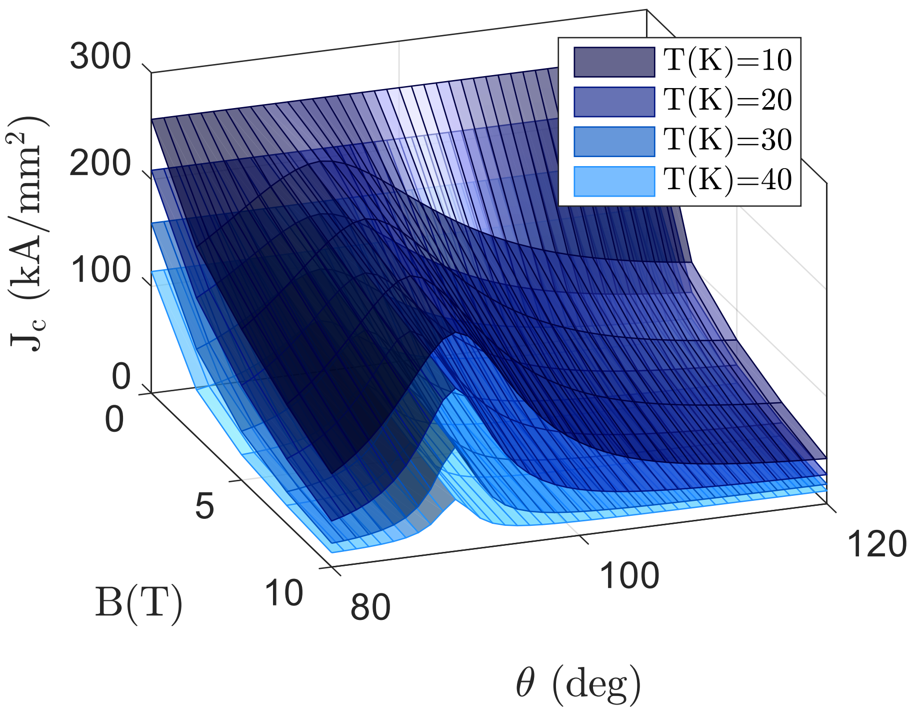

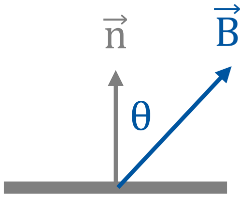

→ Anisotropy included in the model, but uncertainty on material properties

Field Quality Assessment

Pre-cycle → first magnetization

Steps of 250 A, plateaus of 120 s:
decay of inductive effects

Evaluation points $\{p_{i,up}, p_{i,dn}\}$

1. FEM simulation

2. Magnetic field quality calculation

3. Persistent screening currents contribution:

   Calculation of change in magnetic field quality (assuming screening currents as dominant mechanism)

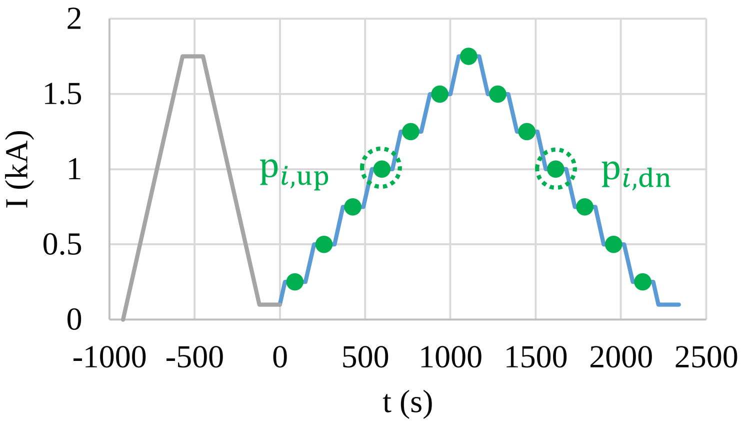

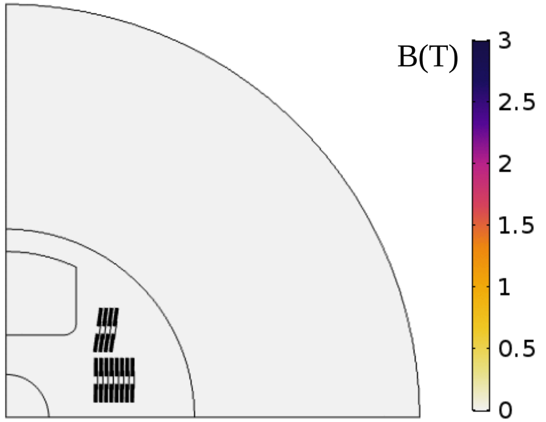

Total magnetic flux density (T),
1 quadrant

Results – FEM Simulation

Current density distribution in the coil:

Same external current, different time steps

Computational time: 120k DoF, 0.9 h (*)

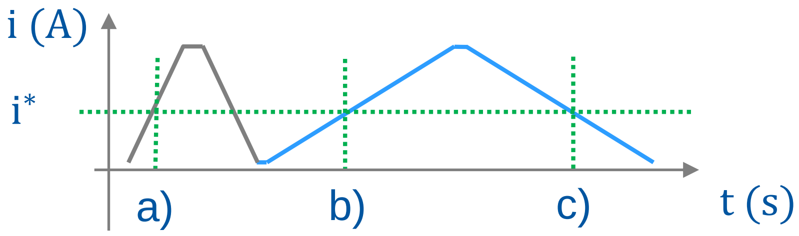

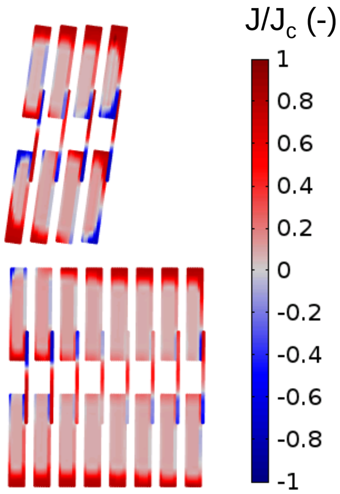

a)

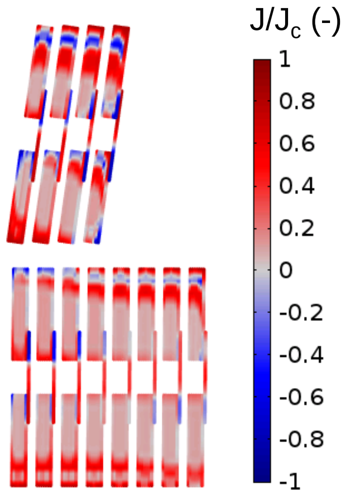

b)

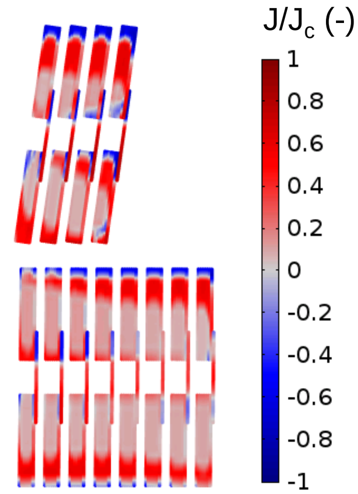

c)

Normalized current density in the coil, shown for the first quadrant

(*) CPU: Intel Core i7-3770 @ 3.40GHz. RAM: 32 Gb. OS: Win 10

Validation – 4. Magnetic Field Quality

b_i field multipoles, as function of the normalized staircase time

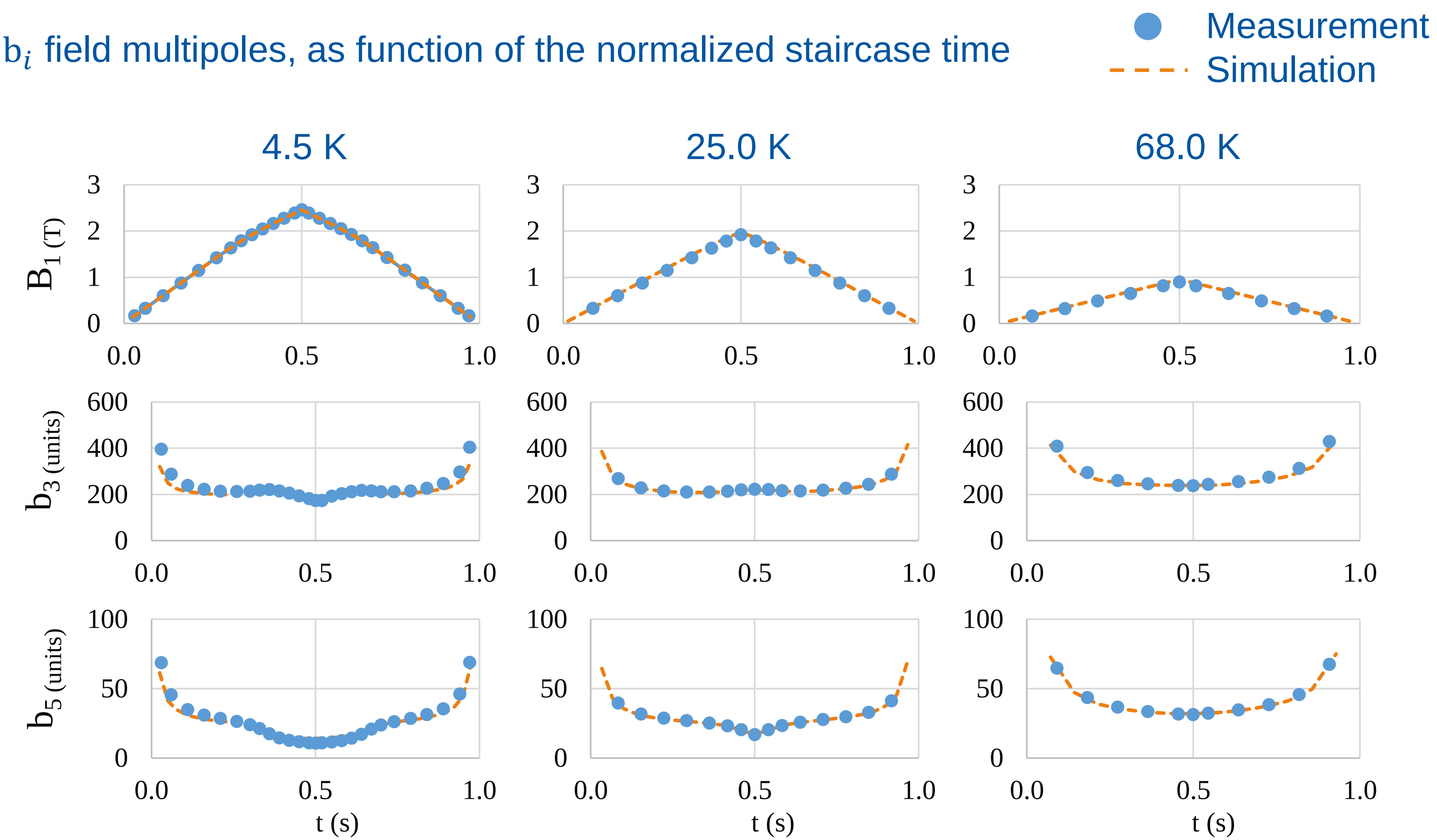

→ Very good agreement with measurements

Validation – 5. Screening Currents

Δb_i field multipole variations, as function of current (in kA)

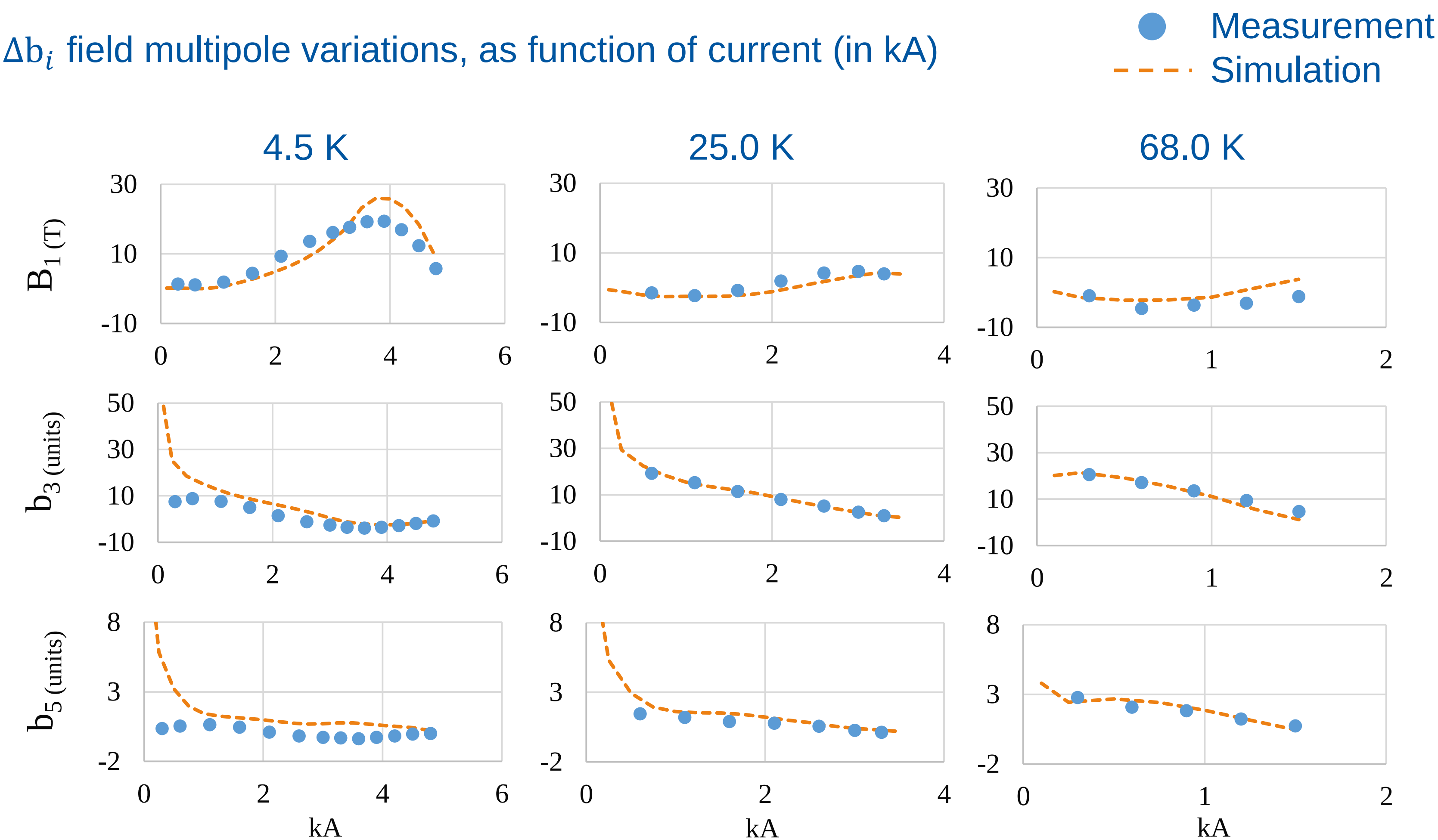

→ Good agreement with measurements, considering uncertainty in $J_c(T, B, \theta)$

Summary and Outlook

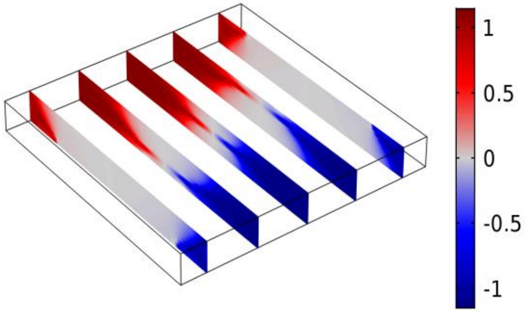

Summary

$\vec{A}$-$\vec{H}$ weak formulation for FEM:

1. Excellent agreement with theory
2. Consistency with Feather2 measurements
3. Stable, scalable and fast (few hours for ~10^4 tapes in 2D models)

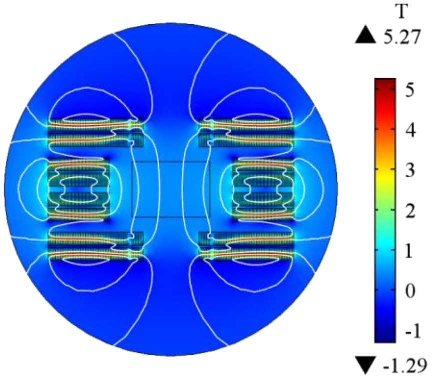

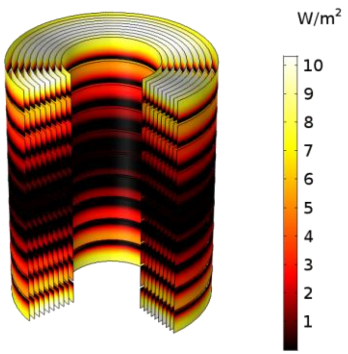

Outlook

1. Include heat balance equation
2. Develop field-circuit coupling interface
3. Include the models in the STEAM co-simulation framework

- Run field quality analysis and optimization
- Run quench protection studies (e.g., Feather2 in FRESCA2)

Thank you for your attention!

TECHNISCHE UNIVERSITÄT DARMSTADT

References

1. Bíró, O. "Edge element formulations of eddy current problems." *CMAM* 169.3-4 (1999): 391-405.

2. Carpenter, C. J. "Comparison of alternative formulations of 3-dimensional magnetic-field and eddy-current problems at power frequencies." *Proceedings of the Institution of Electrical Engineers*. Vol. 124. No. 11. IET Digital Library, 1977.

3. Brambilla, R., Grilli, F., Martini, L., Bocchi, M., & Angeli, G. (2018). A finite-element method framework for modeling rotating machines with superconducting windings. *IEEE Transactions on Applied Superconductivity*, *28*(5), 1-11.

4. Zhang, H., et al. "An efficient 3D finite element method model based on the T–A formulation for superconducting coated conductors.“ *SuST*, 30.2 (2016): 024005

5. Schöps, S., et al. "Winding functions in transient magnetoquasistatic field-circuit coupled simulations." *COMPEL: The International Journal for Computation and Mathematics in Electrical and Electronic Engineering* 32.6 (2013): 2063-2083

6. Russenschuck, S. *Field computation for accelerator magnets: analytical and numerical methods for electromagnetic design and optimization*. John Wiley & Sons, 2011.

7. Knoepfel, H. E., Magnetic fields: a comprehensive theoretical treatise for practical use. John Wiley & Sons, 2008

8. Brandt, E H., "Superconductors of finite thickness in a perpendicular magnetic field: Strips and slabs." *Physical review B* 54.6 (1996): 4246

9. Van Nugteren, J., et al. "Powering of an HTS dipole insert-magnet operated standalone in helium gas between 5 and 85 K." *SuST* 31.6 (2018): 065002.

CERN

Annex

…Why HTS?

Circular accelerators for particle physics:

circular orbit $\mathbf{F}_{\mathrm{Lorentz}} = -\mathbf{F}_{\mathrm{centripetal}}$

$$q(\mathbf{v} \times \mathbf{B}) = -\frac{mv^2}{\mathbf{r}} \,(N) \quad \rightarrow \; r = \frac{mv^2}{qvB} \,(T)$$

$$r_{[km]} \approx 3 \, \frac{p_{\,[TeV/c]}}{B_{[T]}}$$

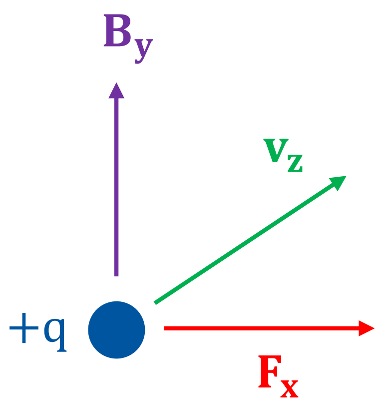

Just for fun

LHC tunnel + HTS dipoles everywhere @ 4.2 K, 30 T:

$$p \approx \frac{1}{3} \cdot \frac{27}{2\pi} \cdot 30 \; \approx 40 \; [TeV/c]$$

Collision energy of the Future Circular Collider (FCC): $p = 50 \; [TeV/c]$

… not so far away after all!

Verification – Current dependency

Scenario: AC loss due to screening currents

$1 < n < \infty, \; J_c = J_{c0}$

$\rightarrow$ ρ as power law

Geometry: single tape

Source: External current I_s

Reference: previous work, e.g. [ref1]:

if $I_s < I_c$: $Q_{AC} \propto I_s^{\,3}$

if $I_s > I_c$: $Q_{AC} \propto I_s^{\,n+1}$
field fully penetrated, J const

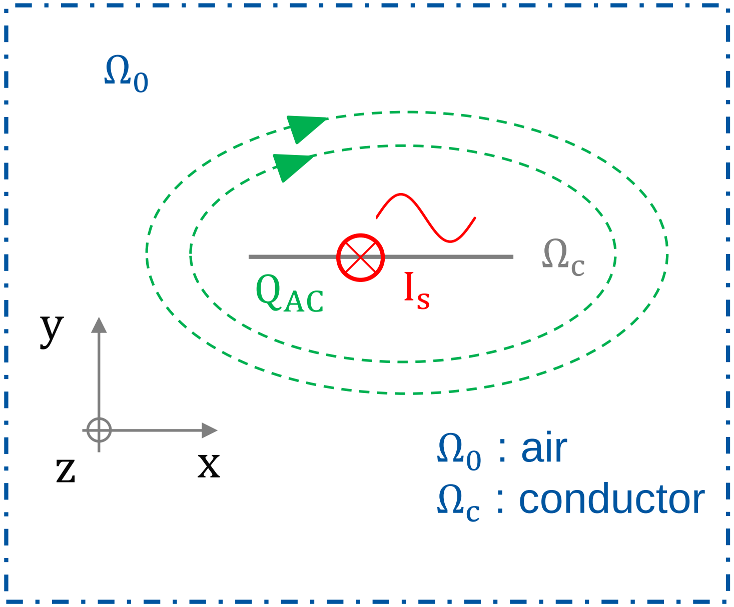

Computational domain

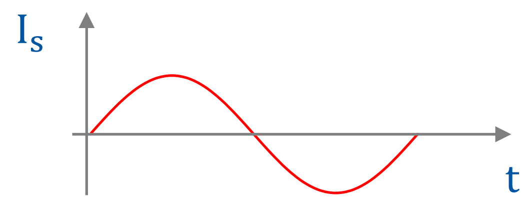

Source term

[ref1] Grilli, F. et al. "Computation of Losses in HTS Under the Action of Varying Magnetic Fields and Currents." IEEE Transactions on Applied Superconductivity 24.1 (2014): 78-110.

Verification – Current dependency

Solution of the transport + screening currents problem

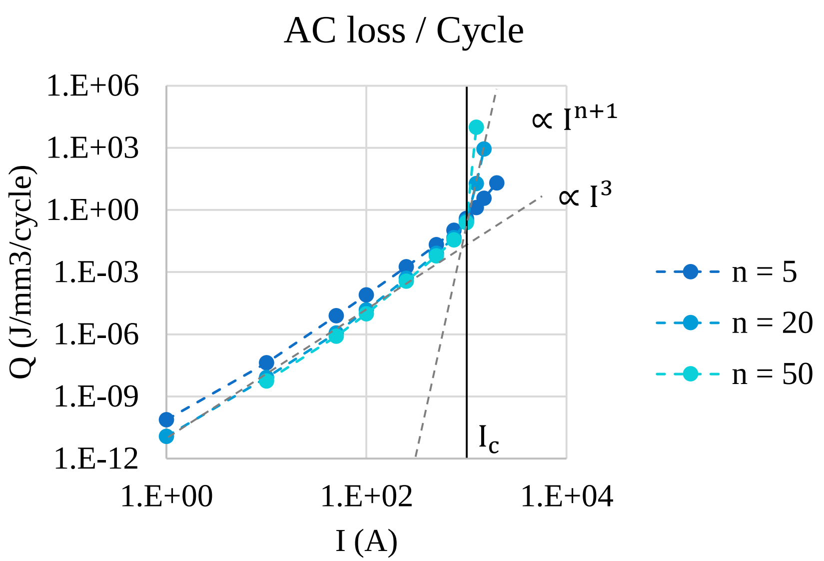

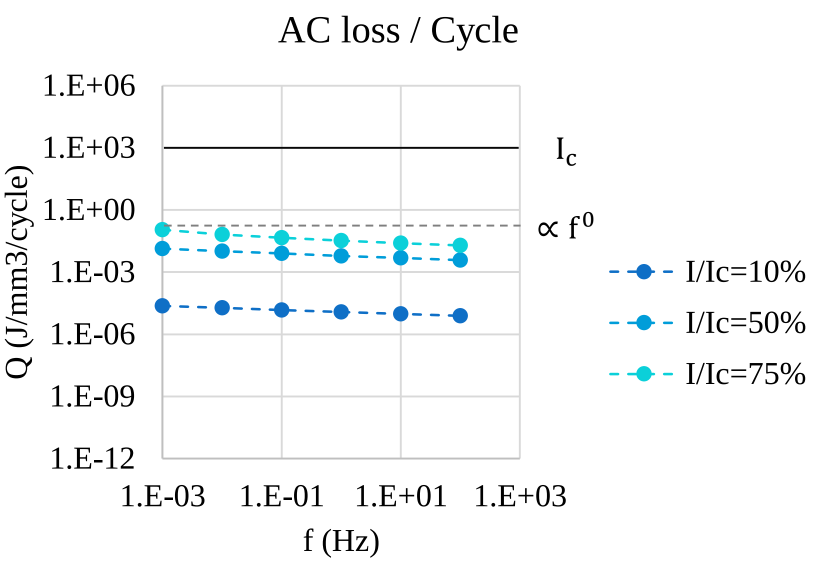

Ac loss per cycle, as function of the applied current. Trends are highlighted with dashed lines

Ac loss per cycle, as function of frequency, for $I < I_c$. Trends are highlighted with dashed lines

→ Consistent with previous research

CERN
TECHNISCHE UNIVERSITÄT DARMSTADT

Magnetic field dynamics in superconductors

Type I: Meißner Effect

- Thermodynamical state, reversible
- London equation

$$\Delta\vec{B} - \lambda^{-2}\vec{B} = 0, \quad \text{if } B < B_{c1}$$

Type II: Abrikosov fluxons

- Flux pinning and motion, irreversible
- Power-law (phenomenological)

$$\rho(\vec{B},T) = \frac{E_c}{J_c(\vec{B},T)}\left(\frac{J}{J_c(\vec{B},T)}\right)^{n-1}$$

- Faraday Law (eddy currents)
-

$$\Delta\vec{H} - \mu\rho^{-1}\partial_t\vec{H} = 0$$

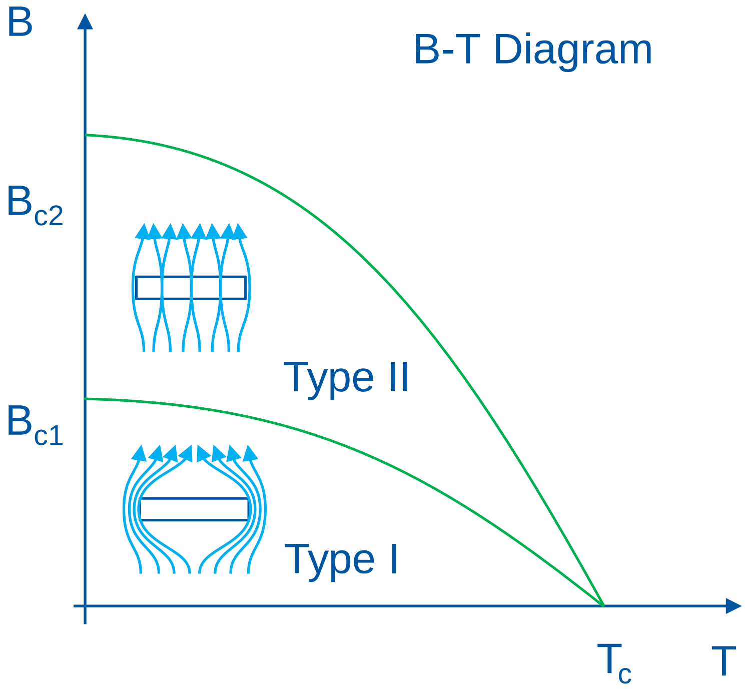

Formulation - Mixed potentials

$\vec{A} - \vec{H}$ formulation, weak form:

1. $\Omega_0 \rightarrow$ Ampere-Maxwell Law
2. $\Omega_c \rightarrow$ Faraday Law
3. $\Omega_c \rightarrow$ Constraint on transport current

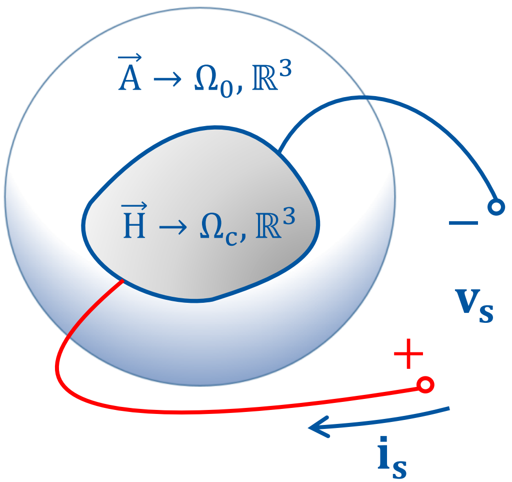

$$\begin{array}{l} 1. \\ 2. \\ 3. \end{array} \begin{bmatrix} \mathbf{M}_\nu & -\mathbf{Q} & \mathbf{0} \\ -\mathbf{Q}^{\mathrm{T}}\partial_t & \mathbf{M}_\rho + \mathbf{M}_\mu \partial_t & \mathbf{X} \\ \mathbf{0} & \mathbf{X}^{\mathrm{T}} & \mathbf{0} \end{bmatrix} \cdot \begin{bmatrix} \mathbf{a} \\ \mathbf{h} \\ v_s \end{bmatrix} = \begin{bmatrix} \mathbf{0} \\ \mathbf{0} \\ i_s \end{bmatrix}$$

$$M^{\nu}_{i,j} = \int_\Omega \mu^{-1} \nabla \times \vec{w}_i \cdot \nabla \times \vec{w}_j \; d\Omega,$$ $\mathbf{M}_\nu$ reluctance

$$Q_{i,q} = \int_\Gamma \vec{w}_i \cdot (\vec{z}_q \times \vec{n}) \; d\Gamma,$$ $\mathbf{Q}$ current

$$M^{\rho}_{p,q} = \int_\Omega \rho \nabla \times \vec{z}_p \cdot \nabla \times \vec{z}_q \; d\Omega,$$ $\mathbf{M}_\rho$ resistance

$$M^{\mu}_{p,q} = \int_\Omega \mu_0 \vec{z}_p \cdot \vec{z}_q \; d\Omega,$$ $\mathbf{M}_\mu$ flux

$$X_p = \int_\Omega \vec{\chi} \cdot \nabla \times \vec{z}_p \; d\Omega.$$ $\mathbf{X}$ voltage

Advantages

$M_\rho(\rho) \rightarrow$ finite conditon number

$\vec{A} \rightarrow$ magnetostatic problem

Drawback

Weak form to be implemented

High-Temperature Superconductors

Cuprate compounds (CuO_2) doped with rare earth elements (La, Bi-Sr-Ca, Y-Ga-Ba …)

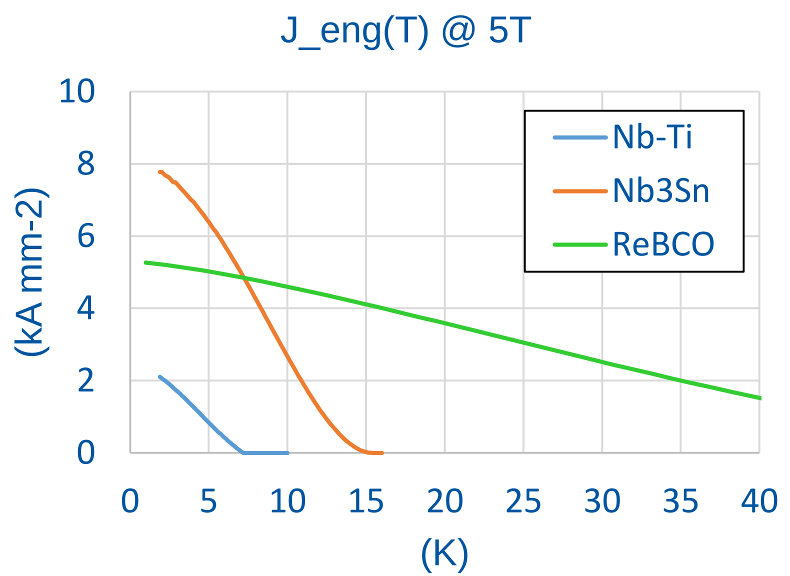

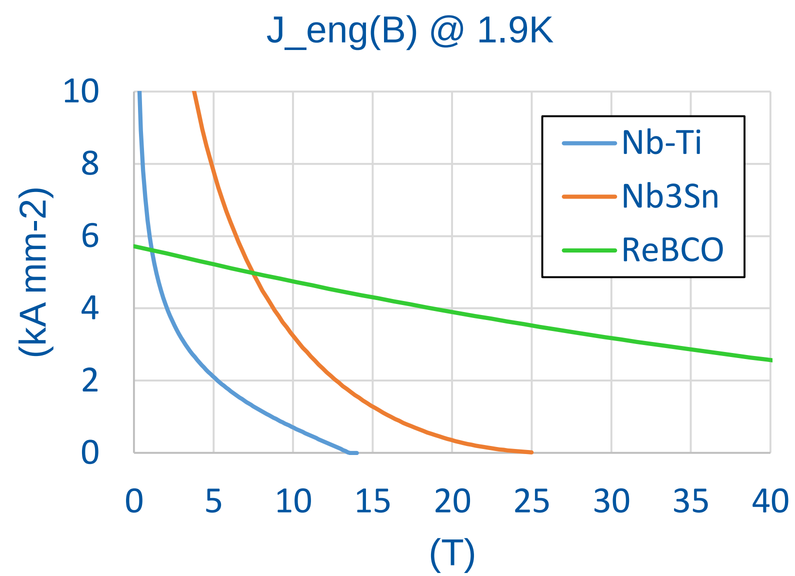

- Higher Tc and Bc0 respect to the traditional LTS competitors
- Higher performance comes with higher prices! $\$_{\mathrm{HTS}} \approx 1e^2\ \$_{\mathrm{LTS}}$

.. But in the early 2000s it was $\approx 1e^3$

Tapes and Cables

Tapes

- ReBCO - Rare Earth Barium Copper Oxide tape
- Batches of $\sim 10^2$ m and beyond
- Cost driven by production process

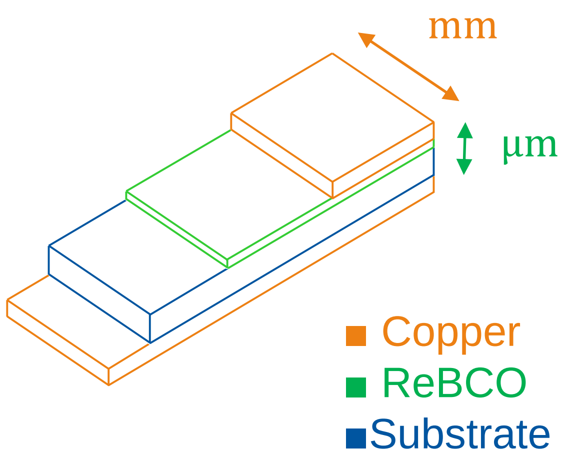

Features

- Multi-layer, multi material
- Aspect ratio ~10^2 (tape), ~10^3 (HTS layer)
- HTS as anisotropic, nonlinear mono-filament $J_c(\vec{B}, T)$
- AC losses: eddy currents

Cables

- Roebel geometry (1912)
- “Coil-able”, bended on the long edge
- Fully transposed: even current distribution
- Aligned-coil concept against AC losses

Source: CDS. Coiled Roebel cable (Henry Barnard, CERN).

Formulation - PEC Limit Behavior

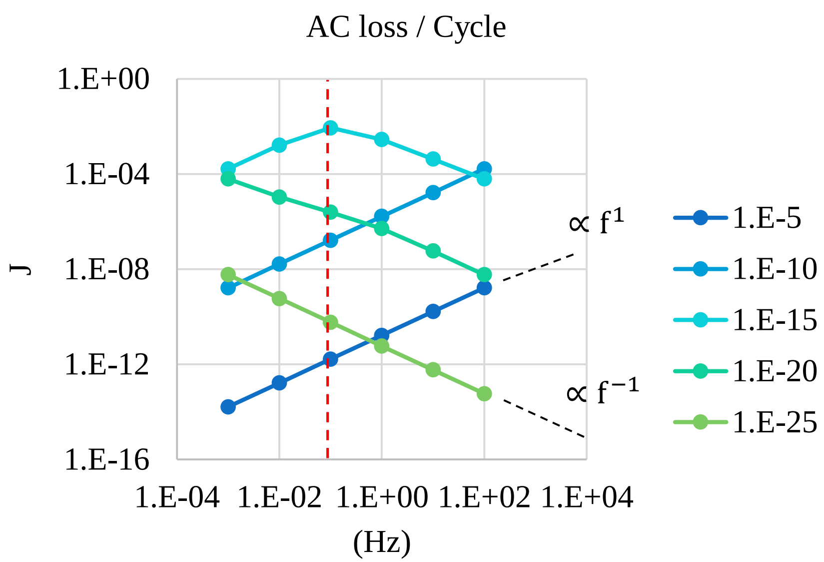

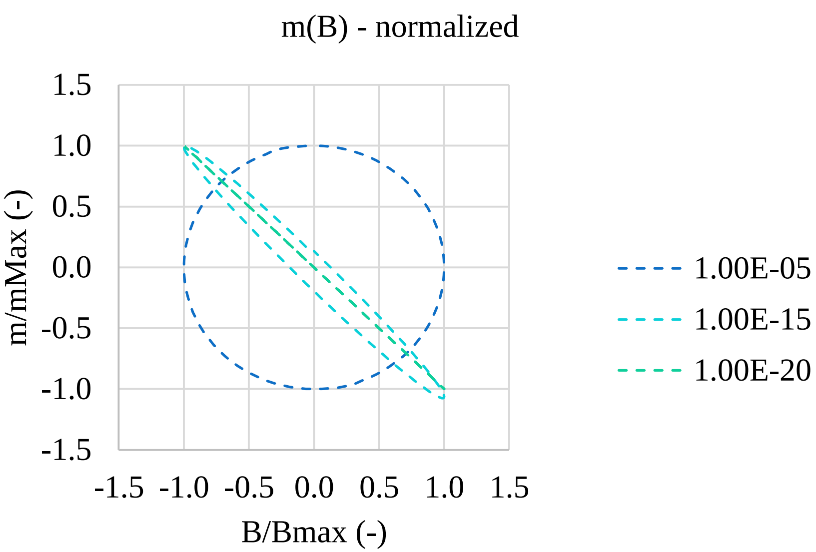

[1] Knoepfel, Heinz E. *Magnetic fields: a comprehensive theoretical treatise for practical use*. John Wiley & Sons, 2008.

Field multipoles without eddy currents

Staircase Scenario at 4.5 K

- “Eddy” considers the HTS tape dynamics
- “No Eddy” assumes a homogeneous current density in the tapes

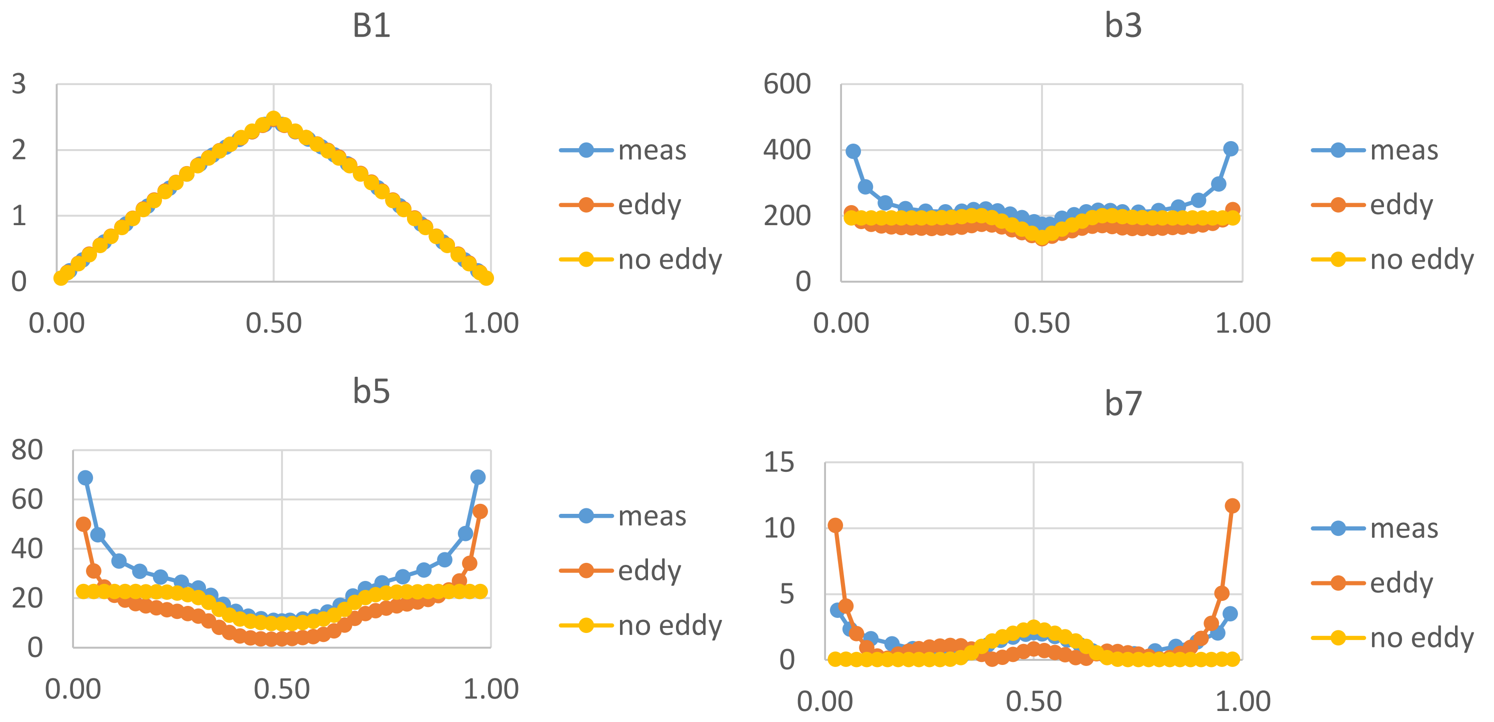

TECHNISCHE UNIVERSITÄT DARMSTADT

Main Differences

Cable architecture:

- LTS – filamentary compound
- HTS – multi-layer tape

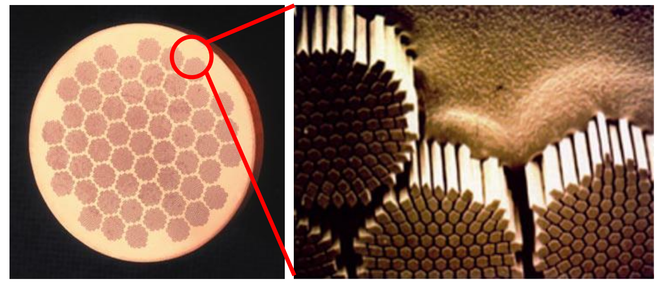

CERNcourier.com

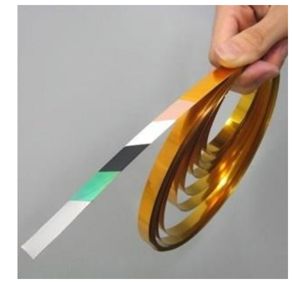

www.fujikura.co.uk

Resistivity ρ: power law

$$\rho = \frac{E_c}{J_c}\left(\frac{J}{J_c}\right)^{n-1}$$

- $n_{LTS} \approx 40, n_{HTS} \approx 20$
- $J_{c,HTS}$ anisotropic

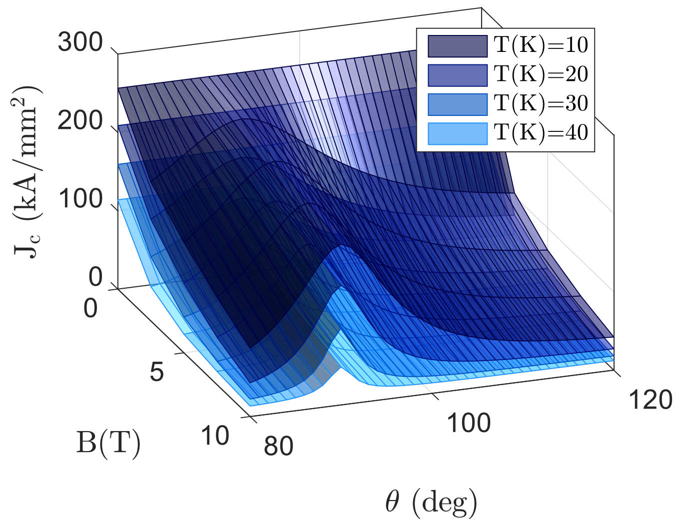

$J_c(T, B, \theta)$

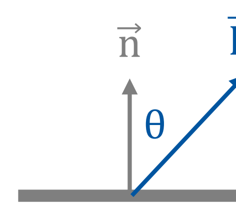

Tape cross section

Formulations

Conditivity σ – based:

- $\vec{\mathbf{A}}$**:** magnetic vector potential
  ill-conditioned mass-conductivity matrix (∞ condition number)

Resistivity ρ – based:

- $\vec{\mathbf{H}}$**:** magnetic field strength
  $\rho \neq 0$ everywhere, unphysical eddy currents , computationally inefficient
- $\vec{\mathbf{T}}$**-**$\boldsymbol{\Omega}$**:** current vector potential-scalar magnetic potential
  cohomology basis functions for net currents in multiply connected domains

Mixed fields (from literature)

- $\vec{\mathbf{A}}$**-**$\vec{\mathbf{H}}$**:** magnetic vector potential + magnetic field strength
  Developed for 2D rotating machinery. Current driven, no external coupling
- $\vec{\mathbf{T}}$**-**$\vec{\mathbf{A}}$**:** current vector potential + magnetic vector potential
  Current driven, no external coupling, suitable only for slabs